ELSEVIER

Surface Science 442 (1999) 90–106

surface science

www.elsevier.nl/locate/susc

Mechanism of the hydrogenation of CO_2 to methanol on a Cu(100) surface: dipped adcluster model study

Zhen-Ming Hu [a,1], Kunio Takahashi [a], Hiroshi Nakatsuji [a,b,*]

[a] *Department of Synthetic Chemistry and Biological Chemistry, Graduate School of Engineering, Kyoto University, Sakyo-ku, Kyoto 606-8501, Japan*

[b] *Institute for Fundamental Chemistry, 34-4 Takano-Nishihiraki-cho, Sakyo-ku, Kyoto 606, Japan*

Received 16 October 1998; accepted for publication 12 August 1999

Abstract

The mechanism of the hydrogenation of CO_2 to methanol on a Cu(100) surface was studied using the dipped adcluster model (DAM) combined with ab initio Hartree–Fock (HF) and second-order Møller–Plesset (MP2) calculations. The Langmuir–Hinshelwood (LH) mode, which corresponds to the reaction between coadsorbed species on the surface, was adopted. Our calculations show that hydrogen and formate are adsorbed at short-bridge sites. The coadsorption of hydrogen and CO_2, in which CO_2 is chemisorbed in the bent anionic state, is described well by the DAM. Five successive hydrogenations are involved in the hydrogenation of adsorbed CO_2 to methanol: the intermediates are formate, dioxomethylene, formaldehyde and methoxy. The geometries of these intermediates and the transition states, as well as the energy diagrams in the reaction process, are presented. The rate-limiting step is the hydrogenation of adsorbed formate. Subsequent steps occur relatively readily, and lead to the formation of methanol. Clearly, any factor that could enhance the hydrogenation of formate on copper should lead to enhanced activity in methanol synthesis.

Keywords: Ab initio quantum chemical methods and calculations; Carbon dioxide; Catalysis; Chemisorption; Copper; Hydrogen; Methanol; Surface chemical reaction

1. Introduction

The hydrogenation of CO_2 to methanol on a copper-based catalyst is one of the most extensively studied industrial processes, since it is promising not only with regard to the use of CO_2 [1,2], but also because methanol is a key material for the synthesis of other organic materials, such as formaldehyde, alkyl halides and acetic acids. Industrially, methanol is now made catalytically from synthesis gas containing carbon monoxide, carbon dioxide and hydrogen in the presence of a $Cu/ZnO/Al_2O_3$ catalyst [2]. Because of its industrial importance, a great deal of research has been carried out to understand the mechanism of this reaction [3–23], with the aim of identifying a highly active and selective catalyst for methanol synthesis.

Although a satisfactory mechanism has not yet been worked out, it is assumed that the primary source of the carbon in methanol is CO_2 [3–5],

* Corresponding author. Fax: +81-75-753-5910.
E-mail address: hiroshi@sbchem.kyoto-u.ac.jp (H. Nakatsuji)
[1] Present address: Department of Chemistry, Dalhousie University, Halifax, Canada, B3H 4J3.

0039-6028/99/$ – see front matter
PII: S0039-6028(99)00900-0

and that formate is the pivotal intermediate for methanol synthesis [5,14]. The role of ZnO in this catalytic reaction has been the subject of long-standing debate. Early studies proposed that the Cu^{n+} induced by ZnO was the active site for methanol synthesis [6]. This suggestion still receives some support [7–11]. On the other hand, other studies support a model which assumes that the active site on the Cu/ZnO catalyst is metallic Cu [12–16], since the activity is directly proportional to the surface area of copper. Recently, attempts have been made to synthesize methanol from H_2 and CO_2 on clean Cu(100) and Cu(110) single-crystal surfaces [17–21]. Methanol was synthesized in these studies, which offers a basis for studies of this reaction on copper-based catalysts.

Evidence for the existence of the formate species has been derived from both infra-red (IR) [22] and temperature-programmed desorption (TPD) spectra of a supported copper catalyst exposed to synthesis gas [23]. Bowker et al. [23] demonstrated that the coadsorption of hydrogen and carbon dioxide on copper resulted in the formation of formate species. Millar et al. [5] further concluded that the copper formate species, which is adsorbed in the bridge form, is a precursor to methanol production. The formate species is known to be readily generated on copper from CO_2 and H_2 under typical methanol synthesis conditions, and has also been synthesized from CO_2/H_2 on Cu(100) and Cu(110) single-crystal surfaces [24,25]. Formate was concluded to be oriented with its molecular plane perpendicular to the metal surface [26], with the two oxygen atoms positioned on top of two equivalent copper atoms. Theoretical calculations also support this observation [27–29].

In methanol synthesis, several hydrogenation steps, such as the hydrogenation of CO_2, formate and further adsorbed intermediates, are involved in the actual reaction process. To clarify the mechanistic details, considerable effort has been devoted to identifying the intermediates in the reaction route and to clarifying the rate-limiting step [5,14,18–21]. However, possible intermediates other than formate, such as dioxomethylene, formaldehyde and methoxy, have not been observed directly by experimental methods. Burch et al. [14] indicated that dioxomethylene is a possible intermediate, and that the critical rate-limiting step in methanol synthesis is the addition of the first hydrogen atom to copper formate. Millar et al. [5] also support this conclusion. On the other hand, Chorkendorff and co-workers [18,19] suggested that the hydrogenation of dioxomethylene may be the rate-limiting step. The hydrogenation of formate and the hydrogenation of methoxy are also possible candidates for the rate-limiting step [19]. Since several hydrogenation reactions are involved, and the lifetime of the intermediates may be short, experimental observation is difficult in the actual continuous reaction process. Theoretical research should play an important role in clarifying the mechanism of this complicated surface reaction process. However, to the best of our knowledge, no full theoretical study has been reported on this subject, although Kakumoto [11] discussed the reaction route based on a cluster model which contained just one or two copper atoms.

In this study, we examined the mechanism of the hydrogenation of CO_2 to methanol on a Cu(100) surface by the dipped adcluster model (DAM) [30] combined with the ab initio Hartree–Fock (HF) and second-order Møller–Plesset (MP2) methods. The DAM has been successfully applied to the chemisorption of oxygen on palladium and silver surfaces [31–35]. Recently, the mechanisms of the epoxidation and complete oxidation of ethylene [36,37] and propylene [38,39] on a silver surface were clarified using the DAM. A comparative study of the epoxidation of ethylene on copper, silver and gold surfaces has also been carried out [40]. Section 2 gives an outline of the computational details. The overall reaction mechanism in methanol synthesis and the geometries and energetics of the elementary steps are reported in Sections 3 and 4, respectively. In Section 5, the adsorption of atomic hydrogen and formate, as well as the coadsorption of hydrogen and CO_2, on a Cu(100) surface are discussed. Finally, we give the conclusions from the present study in Section 6.

2. Computational details

A $Cu_8(6,2)$ cluster, which contains six copper atoms in the first layer and two copper atoms in

the second layer, as shown in Fig. 1, was used to model the Cu(100) surface. The dipped adcluster model (DAM) [30] was used to include the effects of the bulk metal, such as electron transfer between the admolecule and the surface, and the image force. The calculations were performed using the highest-spin coupling model [30] and so one-electron transfer from the bulk metal was assumed [30–32].

The Langmuir–Hinshelwood (LH) mode, which corresponds to the reaction between the coadsorbed species on the surface, was adopted. This is reasonable since hydrogen is dissociatively adsorbed on the Cu(100) surface and the coadsorbed species is responsible for methanol formation [14,24]. The detailed reaction mechanism in the hydrogenation of adsorbed CO_2 to methanol was studied by choosing the appropriate reaction coordinates of the bridge site. The chemisorption of atomic hydrogen and formate as well as the coadsorption of hydrogen and CO_2 were also investigated, and the results were compared with available experimental and theoretical data.

The geometries of the reactants, products and intermediates were optimized at the HF level, except for the Cu—Cu distance, which was fixed at its bulk lattice value of 2.556 Å. The geometries of the transition states (TSs) were calculated using the force constant matrix at the HF level; namely, the energy gradient was zero and the force constant matrix had only one negative eigenvalue at the TS. The electrostatic interaction energy between the adcluster and the bulk metal was estimated by image force correction [31]. Electron correlations were included by the MP2 method. The calculations were performed with the GAUSSIAN 94 software package [41].

The Gaussian basis set for the copper atom was the (3s2p5d)/[3s2p1d] set and the argon core was replaced by the effective core potential [42]. For oxygen and carbon, we used the (9s5p)/[4s2p] set of Huzinaga–Dunning [43,44]. For hydrogen, (4s)/[2s] [44] was adopted in HF optimization calculations. In MP2 calculations, the polarization *d* function of $\alpha = 1.154$ and 0.60 [45] and the polarization *p* function of $\alpha = 1.1$ [41] were added to the oxygen, carbon and hydrogen basis sets, respectively. Test calculations with the present methodology on the gas-phase reactions relative to the present system are shown in Table 1. The calculated results are all in reasonably good agreement with the experimental values.

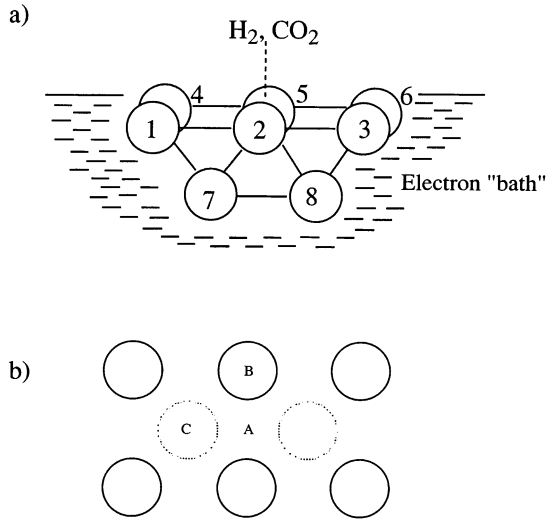

Fig. 1. (a) Side view of the model adcluster used in this study. Cluster atoms 1–6 are in the first layer, and 7 and 8 are in the second layer. (b) Top view of the adsorbed bridge (A), on-top (B) and hollow (C) sites. The solid and dashed circles denote the first and second layers, respectively.

3. The overall reaction mechanism in methanol synthesis

The main purpose of the present study was to understand the mechanistic details of the hydrogenation of CO_2 into methanol on a Cu(100) surface. Since this is a very complicated process, we focused on clarifying the reaction intermediates, the transition states and the energetics of the important hydrogenation reaction steps. We then determined the overall reaction mechanism as well as the rate-limiting steps. The most important results and discussions are summarized in this section, and the detailed geometries and energetics of each elementary step are shown in the next section.

The elementary reaction steps on the surface

Table 1
Calculated and experimental properties for the gas-phase reactions[a]

Reaction	R_e (Å)			D_e (kcal mol^{-1})	
	HF	MP2	Experimental[b]	MP2	Experimental[b]
$H+H\rightarrow H_2$	0.731	0.736	0.741	101.9	103.3
$O+O\rightarrow O_2$	1.207	1.238	1.2075	117.3	118.0
$Cu+H\rightarrow CuH$	1.587	1.535	1.572	66.6[c]	63.0
$H_2+CO_2\rightarrow CH_3OH+H_2O$				15.9[d]	14.9[e]

[a] R_e — bond length; D_e — binding energy.
[b] Ref. [67].
[c] Calculated value of 44.3 kcal mol^{-1} relative to the $Cu(^2S)+H(^2S)$ ground-state limit plus the energy difference of 22.3 kcal mol^{-1} [68] between $Cu(^2S)$ and $Cu(^2D_{5/2})$ states, since the experimental value [67] is relative to the $Cu(^2D_{5/2})+H(^2S)$ limit.
[d] Heat of reaction.
[e] Ref. [69].

can be summarized as follows:

$$H_2(g)\rightarrow 2H(a) \quad (1)$$

$$CO_2(g)\rightarrow CO_2(a) \quad (2)$$

$$CO_2(a)+2H(a)\rightarrow HCOO(a)+H(a) \quad (3)$$

$$HCOO(a)+H(a)\rightarrow H_2COO(a) \quad (4)$$

$$H_2COO(a)+H(a)\rightarrow H_2CO(a)+OH(a) \quad (5)$$

$$H_2CO(a)+H(a)\rightarrow H_3CO(a) \quad (6)$$

$$H_3CO(a)+H(a)\rightarrow CH_3OH \quad (7)$$

$$OH(a)+H(a)\rightarrow H_2O \quad (8)$$

Among these elementary reactions, steps (3)–(7) constitute the core steps in methanol synthesis, and the overall reaction energetics are shown in Fig. 2. The energy diagram shown in Fig. 2 is composed of the energetics of the elementary reaction steps; i.e., they are calculated separately. The numbers of atoms in steps (3) and (4) are identical, but different in the following steps, so that we put the energy level of the reactant of step (5) to be the same as that of the product of step (4), and similar procedure is done for the next steps (6) and (7), to give an overall energetic understanding of the reaction pathways. An illustration of the reaction mechanism in methanol synthesis proposed by our study is shown in Fig. 3.

Among the hydrogenation steps, the hydrogenation of adsorbed formate to adsorbed dioxomethylene, i.e., step (4), is the rate-limiting step, as shown in Fig. 2. The activation energy in this step is calculated to be 23.0 kcal mol^{-1}, which is higher than that in the other hydrogenation steps. This step is also endothermic by 17.1 kcal mol^{-1}. This result is consistent with the suggestion based on experimental findings that the critical rate-limiting step in methanol synthesis is the addition of the first hydrogen atom to adsorbed formate [5,14,20]. The high energy barrier and an unstable dioxomethylene intermediate account for the lower activity of a clean copper surface as compared with a copper-based catalyst in practical methanol synthesis. Dioxomethylene has been suggested to be an intermediate in methanol synthesis [14,19], but there is no direct experimental evidence to confirm this point. Our optimization calculations show that dioxomethylene is adsorbed on a Cu(100) surface at the bridge site with its molecular plane perpendicular to the metal surface; i.e., an adsorption geometry similar to that of formate adsorbed at the surface.

Another high energy barrier (17 kcal mol^{-1}) is calculated for step (5), the hydrogenation of adsorbed dioxomethylene to give formaldehyde, while this step is exothermic by 35.7 kcal mol^{-1}. Therefore, step (5) may cooperate with step (4) to be rate-limiting, though the former seems be easier than the latter. Experimentally, Chorkendorff and co-workers [18,19] suggested that the former step may be rate-limiting. On the other hand, the decomposition of dioxomethylene

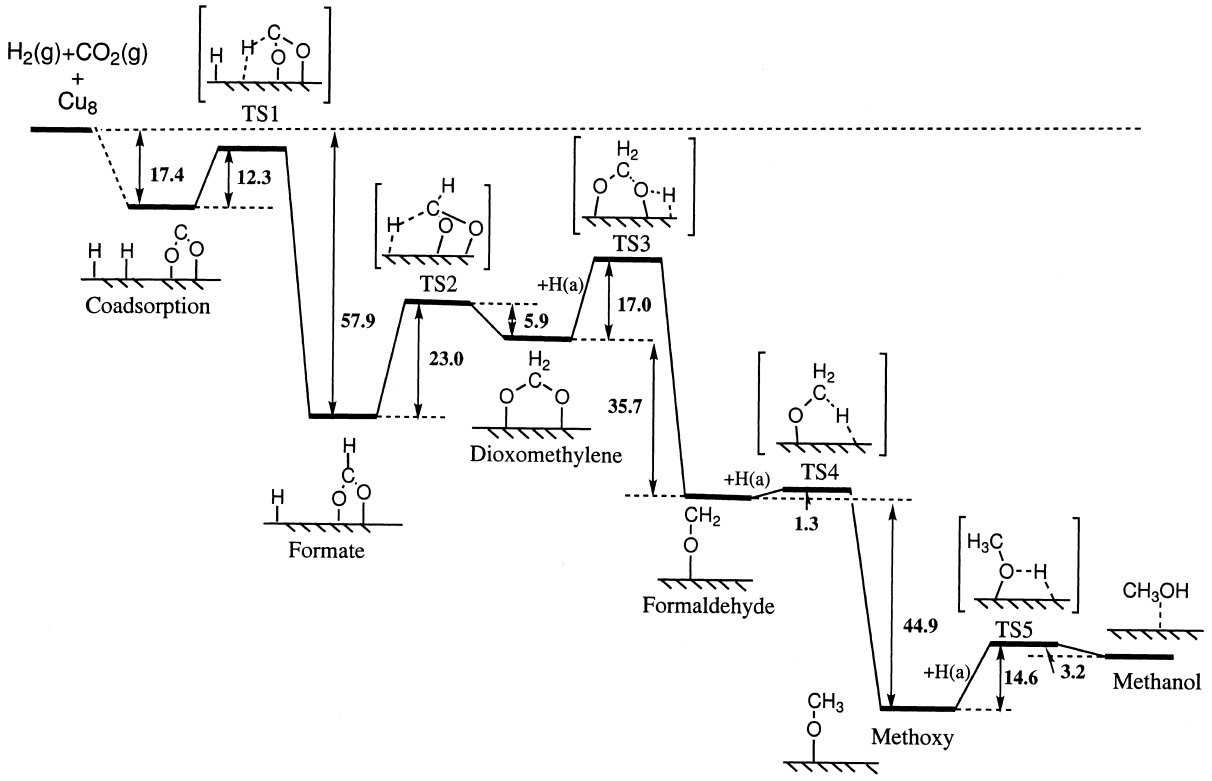

Fig. 2. A summary of the energy diagram for the hydrogenation of CO_2 to methanol on a Cu(100) surface. The geometries and energies of each reaction step are shown in Figs. 4–8. Detailed explanations are given in the text.

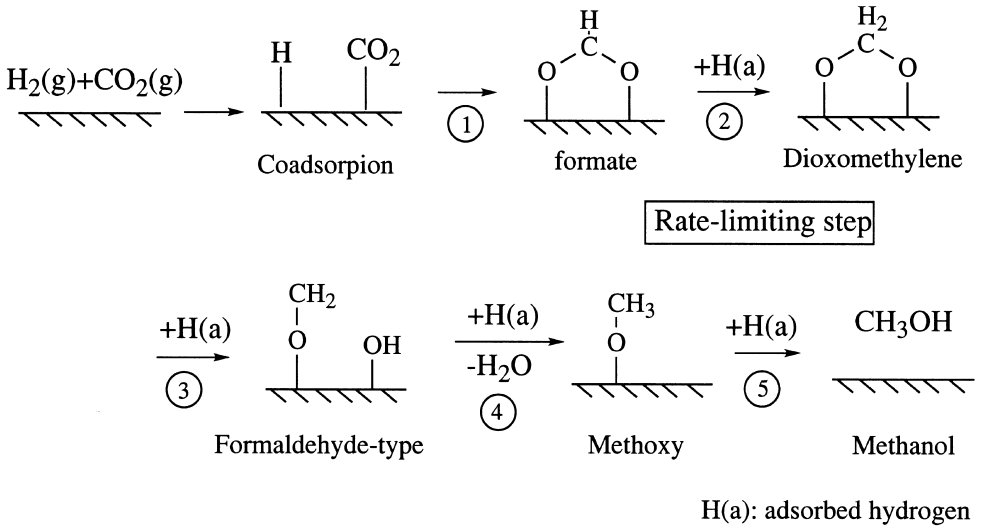

Fig. 3. Proposed reaction mechanism of the hydrogenation of CO_2 to methanol on a Cu(100) surface.

into formate, i.e., the backward reaction, is also favorable: the energy barrier is 5.9 kcal mol^{-1} and the reaction is exothermic by 17.1 kcal mol^{-1}. We can expect that dioxomethylene will decompose into formate in the absence of coadsorbed hydrogen. Thus, step (5) is important for achieving a high selectivity in methanol synthesis. It may be more reasonable to say that the formate to formaldehyde reactions are the rate-limiting steps. Compared with steps (4) and (5), steps (6) and (7) are both easy and rapid, leading to an overall exothermic methanol synthesis.

Table 2 summarizes the calculated vibrational mode with an imaginary frequency at the TSs shown in Fig. 2 and in Figs. 4–8. The TSs have just one negative eigenvalue of the Hessian, and the reaction is mainly related to the reaction mode, as shown by the vibrational modes with large coefficients in the eigenvector. All of these give clear confirmation for the TSs clarified. The energy level of the TSs shown in Fig. 2 is the most important factor in determining the rate-limiting step. The detailed geometries and energetics of the TSs are shown in the next section.

Table 2
Vibrational modes with imaginary frequencies at the TSs given in Figs. 2, 4–8

TS structure	Eigenvalue	Mode	Eigenvector
TS1	−0.057	H_a—x stretching	0.464
		H_a—C stretching	−0.847
		CH_ax torsion	−0.198
		OCH_a torsion	0.135
TS2	−0.088	H_b—x stretching	0.494
		H_b—C stretching	0.425
		CH_bx torsion	0.712
		$H_b$xx torsion	−0.131
		OCH_b torsion	−0.115
TS3	−0.089	H_c—Cu_l stretching	−0.307
		H_c—Ob stretching	0.915
		O_b—C stretching	−0.100
		C—O_a stretching	0.117
		CO_bCu_2 torsion	0.143
		O_bCO_a torsion	0.139
TS4	−0.155	H_c—C stretching	0.906
		H_cCO torsion	−0.333
		C—O stretching	0.119
TS5	−0.122	H_d—x stretching	0.269
		H_d—O stretching	−0.902
		$H_d$xx torsion	0.220
		OH_dx torsion	0.248

Our calculations show that chemisorbed CO_2^-, formate, dioxomethylene, formaldehyde and methoxy are the main intermediates in methanol synthesis, and Eqs. (3)–(7) provide a reasonable reaction route leading to methanol formation on a Cu(100) surface. Surface formate is readily formed by the reaction of adsorbed atomic hydrogen with coadsorbed CO_2, which exists as a bent anionic CO_2^- species, as shown in Section 5. About one electron is transferred from the metal surface to the π^* orbital of CO_2, making the carbon very reactive. Adsorbed formate is easily synthesized from CO_2 and H_2 on a Cu(100) surface [14,24,46], as has been shown experimentally. Adsorbed formate has been confirmed to be a reaction intermediate by IR [5,22] and TPD [23] experiments.

Dioxomethylene, formaldehyde and methoxy have been suggested to be the adsorbed intermediates in surface reactions on copper surfaces by a variety of surface science techniques. Dioxomethylene has been suggested to be an intermediate in the conversion of formaldehyde into formate on an oxidized Cu(110) surface based on X-ray photoelectron spectroscopy (XPS) and TPD [47]. The dissociation of methanol into methoxy has been confirmed by TPD on clean and oxidized Cu(110) [48] and by high-resolution electron energy-loss spectroscopy (HREELS) on Cu(100) [49]. The adsorption of formaldehyde has been observed on Cu(110) [48,49].

Chemisorbed CO_2^- and formate have been reported to be the reaction intermediates by several experimental studies [5,14,22–24,50]. The existence of an adsorbed methoxy intermediate has also been reported by in situ IR studies [51,52]. However, there are no direct experimental reports to confirm that dioxomethylene and formaldehyde are intermediates. Our results show that the adsorbed formaldehyde intermediate is very active, and can be easily hydrogenated into adsorbed methoxy. Dioxomethylene is unstable compared with other intermediates. Further experimental studies are needed to detect these adsorbed intermediates. Charge transfer is the most important feature in this catalytic process.

4. Geometries and energetics of the elementary reaction steps

4.1. Reaction of coadsorbed hydrogen and CO_2^-

As shown in Section 5.2, the coadsorption of hydrogen and CO_2 leads to a bent anionic CO_2^- species on the surface. In coadsorbed CO_2^-, the transfer of one electron from the surface into the π^* orbital of CO_2 causes a large frontier density on the carbon atom, resulting in high reactivity towards coadsorbed hydrogen and leading to the formation of the surface formate species, which is an important intermediate in methanol synthesis [5,14,22–24]. Formate is adsorbed at the short-bridge site on a Cu(100) surface, as shown above and based on other experimental and theoretical studies [26–29]. Fig. 4 shows the optimized geometries and relative energies for the transition state and the intermediate for the reaction path from coadsorbed hydrogen and CO_2^- into the adsorbed formate species on a Cu(100) surface.

The reaction is initiated by the attack of the adsorbed hydrogen atom by the activated carbon atom of the chemisorbed CO_2. The CO_2^- inclines towards the nearest-neighbor adsorbed hydrogen to create an effective overlap to form a C—H σ bond. The optimized geometries show that the C—H bond distance decreases from 2.94 to 1.59 Å, and then to 1.09 Å in the reactant, TS and intermediate, respectively. Meanwhile, the Cu—H distance increases from 1.80 to 1.94 Å, and then to 4.74 Å. The changes in other geometric parameters are small. The activation energy is calculated to be 12.3 kcal mol^{-1}, and the reaction is exothermic by 40.5 kcal mol^{-1}. In this reaction step, the net charges of the adsorbates are calculated to be −0.76, −0.66 and −0.65, respectively, which shows that the reaction process is anionic. An experimental study on the synthesis of adsorbed formate from hydrogen and CO_2 on a Cu(100) surface was reported by Taylor et al. [24], and the activation energy was reported to be 13.3 kcal mol^{-1}, which is in reasonably good agreement with the present result.

4.2. Hydrogenation of adsorbed formate

When formate is formed on the surface, the reaction of coadsorbed formate and hydrogen into dioxomethylene is expected. Fig. 5a shows the coadsorption state at the closest short-bridge sites, which acts as the reactant in this reaction step. The coadsorption state has an adsorption energy similar to that in Fig. 4c. The calculated optimized geometries and relative energies of the transition state and intermediate are shown in Fig. 5.

The reaction path is the attack of the carbon

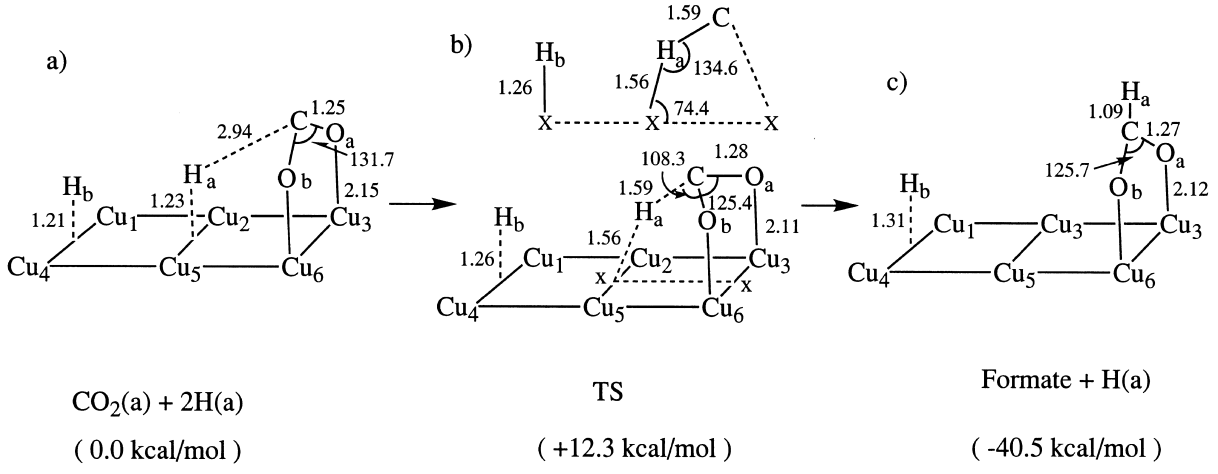

Fig. 4. Optimized geometries and relative energies of the reactant (a), TS (b) and product (c) in the hydrogenation of adsorbed CO_2^-. Bond lengths are in Å and angles are in degrees.

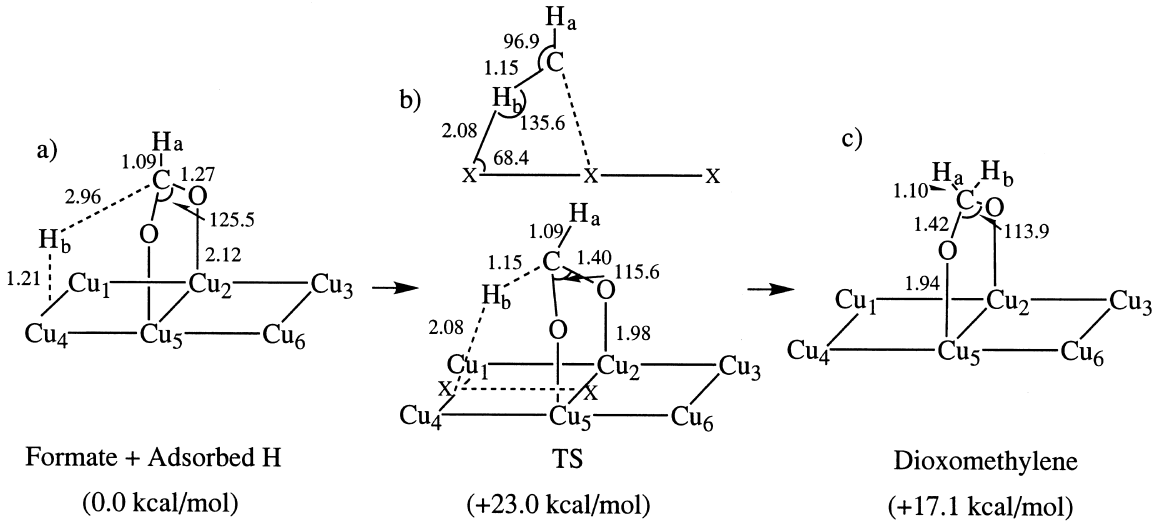

Fig. 5. Optimized geometries and relative energies of the reactant (a), TS (b) and product (c) in the hydrogenation of adsorbed formate.

atom of formate by hydrogen. In the process leading to the TS, the formate inclines towards the adsorbed hydrogen while the adsorbed hydrogen migrates towards the formate, which leads to interaction between the carbon and hydrogen atoms. The Cu—O distances in the reactant, TS and intermediate are 2.12, 1.98 and 1.94 Å, respectively. The C—O distance increases from 1.27 to 1.40 Å, and then to 1.42 Å, and the C—H distance decreases from 2.96 to 1.15 Å, and then to 1.10 Å. In the intermediate state, dioxomethylene has a C—O distance of 1.42 Å and $\angle OCO = 113.9^{\circ}$, which reflect saturated coordination of the carbon atom. The Cu—O distance is 1.94 Å, which is smaller than that (2.12 Å) in the reactant. Electron transfer plays an important role in this step. The net charges of the adsorbates in the reactant, TS and intermediate states are −0.68, −0.93 and −0.96, respectively. On the other hand, no large difference in the relative net charge was found on the cluster side.

The energy barrier for this reaction step is 23.0 kcal mol^{-1}. The experimental activation energy for the hydrogenation of formate was reported to be 19.6 kcal mol^{-1} [53]. The adsorbed dioxomethylene species is 17.1 kcal mol^{-1} less stable than the coadsorbed formate and hydrogen species. Thus, the reaction leading to the formation of dioxomethylene is endothermic. A relatively unstable adsorbed dioxomethylene intermediate on the copper surface may favor further hydrogenation. On the other hand, dioxomethylene may decompose into formate in the absence of coadsorbed atomic hydrogen as stated above; the energy barrier for this decomposition is 5.9 kcal mol^{-1}. The relatively large energy barrier and the unstable intermediate strongly suggest an unfavored reaction path, and a higher temperature is needed to compensate for the energy loss. This unfavored reaction step may explain the lower activity of a clean copper surface in methanol synthesis. Compared with other reaction steps discussed below, the hydrogenation of formate has the highest barrier and the largest endothermic energy. Therefore, we conclude that this is the rate-limiting step, as discussed in Section 3.

4.3. Hydrogenation of adsorbed dioxomethylene

There are two possible reaction pathways for the hydrogenation of adsorbed dioxomethylene. One is the attack of the oxygen atom of adsorbed dioxomethylene by atomic hydrogen, leading to the formation of adsorbed formaldehyde, and the other is attack of the carbon atom by atomic hydrogen, leading to the formation of an adsorbed

bidentate CH_3O_2 species. Since no stable adsorbed CH_3O_2 species was found on a Cu(100) surface in our optimization calculation, the latter pathway can be ruled out. Therefore, we studied the attack of the oxygen atom of adsorbed dioxomethylene by atomic hydrogen.

To simulate a reasonable reaction path, the reaction mode is chosen at the $Cu_1—Cu_2—Cu_3$ side of the Cu_8 cluster, as shown in Fig. 6. An adjacent on-top coadsorbed atomic hydrogen species is taken as the reactant, since coadsorption with atomic hydrogen at the adjacent bridge site does not give a stable minimum. Although coadsorption with hydrogen atoms at a next nearest-neighbor bridge site may be another possibility, it is not a suitable initial reactant due to the large distance between hydrogen and dioxomethylene. On-top atomic hydrogen is a possible candidate for methanol synthesis, since it may exist under perturbation by other coadsorbed species, or as a result of migration from other adsorption sites [14,54]. In this reaction step, adsorbed hydrogen attacks one of the oxygen atoms of dioxomethylene, forming an H—O σ bond. In the TS structure, although the interaction of the hydrogen atom with the oxygen atom is dominant, the interactions of the adsorbates with the surface as well as that of the oxygen atom with the carbon atom are also included (see Table 2). The $C—O_b$ distance is 1.44 Å, which is slightly longer than the $C—O_a$ distance (1.41 Å). All of the distances between the adsorbates and the surface in the TS are longer than in the reactant state. The $H_c—O_b$ distance is 1.54 Å, which reflects the formation of a σ bond. The energy barrier is calculated to be 17.0 kcal mol^{-1}, which is smaller than that in the hydrogenation of adsorbed formate, as discussed above.

The adsorbed formaldehyde and hydroxyl group are the expected intermediates in this reaction path. The structure of this intermediate is shown in Fig. 6c. In the adsorbed intermediate state, formaldehyde has a C—O distance of 1.35 Å, which is comparable to that in the gas phase (1.21 Å). The carbon atom of formaldehyde at the adsorption state should be very reactive towards other coadsorbed hydrogen, and further hydrogenation is expected to occur fairly easily. The adsorbed formaldehyde prefers to occupy the bridge site to have stronger interaction with the surface copper. However, due to repulsive interaction with the adjacent coadsorbed hydroxyl group, the structure deviates from the bridge site. The $Cu_3—O_a$ distance is 1.95 Å, while the $Cu_2—O_a$ distance is 2.30 Å. In addition, the $Cu_1—O_b$ distance of 1.92 Å is shorter than the $Cu_2—O_b$ distance (2.08 Å). This reaction step is calculated to be exothermic by 35.7 kcal mol^{-1}.

Hydroxyl is a well-known radical that is formed in the oxidation of hydrogen and hydrocarbons on the surfaces of transition metals. The disproportionation of two surface hydroxyl groups to produce water and an adsorbed oxygen atom on a silver surface has been discussed previously [55]. The present structure of the hydroxyl group adsorbed on a copper surface is similar to that on

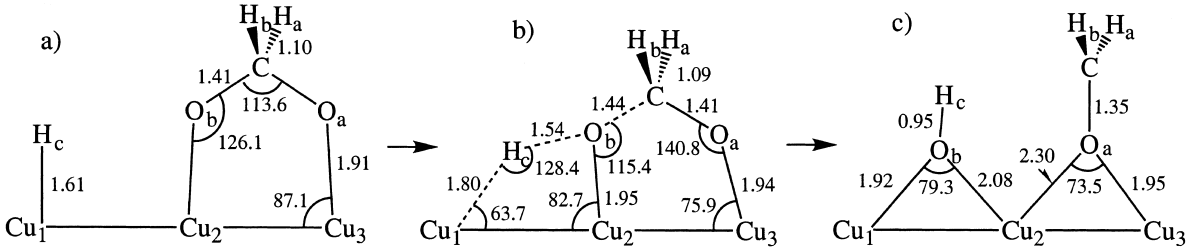

Fig. 6. Optimized geometries and relative energies of the reactant (a), TS (b) and product (c) in the hydrogenation of adsorbed dioxomethylene.

a silver surface produced in the oxidation of olefins [38,39]. However, the disproportionation reaction seems less favorable on a copper surface due to the presence of active adsorbed atomic hydrogen in this reaction process. The adsorbed hydroxyl groups may be converted into water when they react with adsorbed atomic hydrogen.

4.4. Hydrogenation of adsorbed formaldehyde and methoxy

Fig. 7 shows the optimized geometries and relative energies for the hydrogenation of adsorbed formaldehyde into methoxy along the bridge reaction coordinate. The stable coadsorption geometry is that in which formaldehyde is adsorbed at the bridge site, but with the CH_2 fragment slightly inclined towards the surface. The C–O-surface angle is calculated to be 177.2°. The geometry of the formaldehyde side is the same as that of the coadsorbed hydroxyl species, as shown in Fig. 6c. In the TS, the adsorbed formaldehyde species inclines further towards the adsorbed hydrogen to realize an effective interaction between carbon and hydrogen. The optimized geometries show that the C—H bond distance decreases from 3.06 to 1.94 Å, and then to 1.09 Å in the reactant, TS and intermediate, respectively. The activation energy of this step is only 1.3 kcal mol^{-1}. The small activation energy is due to the activity of the unsaturated carbon atom at the adsorption state, which has high reactivity to form another C—H σ bond. The product of this reaction step is adsorbed methoxy, which is 44.9 kcal mol^{-1} more stable than the reactant. Owing to the high activity of the adsorbed formaldehyde intermediate, this reaction step proceeds very smoothly.

When methoxy is formed, it will undergo further hydrogenation to methanol, as shown in Fig. 8. This step involves an H–O reaction mode. The bonding interaction between hydrogen and oxygen will lead to the formation of methanol, the final product of this reaction process. A TS structure, which corresponds to the formation of methanol from coadsorbed hydrogen and methoxy, is shown in Fig. 8b. In this TS, bonding interaction between hydrogen and oxygen is clear. From the reactant to the TS, and then to the product, the O—H_d distance decreases from 3.08 to 1.49 Å, and then to 0.95 Å, and the C—O distance changes from 1.40 to 1.42 Å, and then to 1.45 Å. Typical single H—O and C—O σ bonds are fully formed in the product state. Meanwhile, the stronger H–O bonding interaction results in weak adsorbate–surface interaction. The O—Cu distance increases from 2.05 to 2.16 Å, and then to 2.52 Å along the reaction coordinate, and adsorbed methanol tends to desorb from the surface. This reaction step has

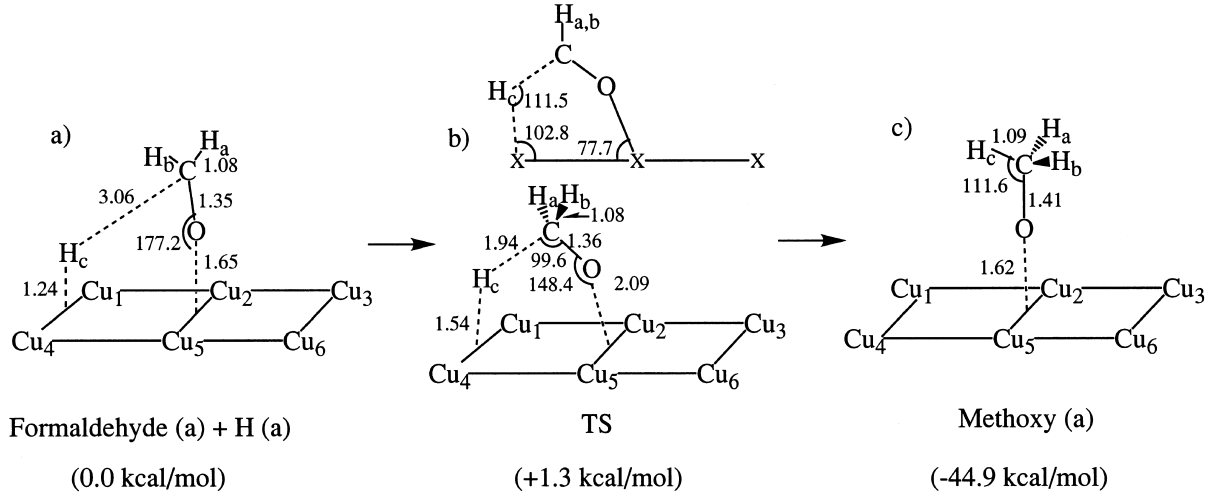

Fig. 7. Optimized geometries and relative energies of the reactant (a), TS (b) and product (c) in the hydrogenation of adsorbed formaldehyde.

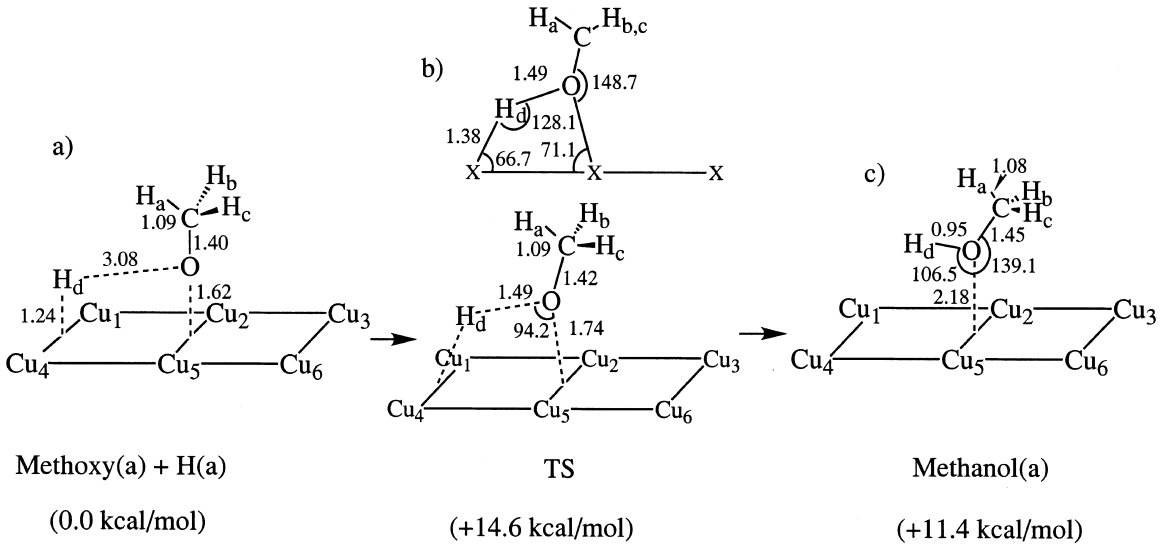

Fig. 8. Optimized geometries and relative energies of the reactant (a), TS (b) and product (c) in the hydrogenation of adsorbed methoxy.

an activation energy of 14.6 kcal mol^{-1}, and is calculated to be endothermic by 11.4 kcal mol^{-1}.

5. Chemisorption of the relevant adsorbates on a Cu(100) surface

In this section, we report comparative studies of the adsorption of hydrogen and formate at different sites on a Cu(100) model cluster, and the coadsorption of hydrogen and CO_2 in the DAM and neutral cluster model, respectively. Although the reaction mechanisms discussed above show little dependence on the results presented here, the adsorptions of these molecules on metal surfaces are of great importance for understanding of molecule–surface interactions and the surface catalytic activities.

5.1. Chemisorption of atomic hydrogen and formate

It is well known that hydrogen is adsorbed dissociatively on a Cu(100) surface [46,56,57], and dissociated atomic hydrogen is responsible for methanol synthesis [18,46,53]. The adsorptions of atomic hydrogen in the bridge, on-top and hollow sites on a Cu(100) surface were examined using the Cu_8 neutral cluster, and the results are compared in Table 3. In the optimized geometries for atomic hydrogen adsorbed in the bridge, on-top and hollow sites, hydrogen was calculated to be 1.64, 1.32 and 1.10 Å above the surface, and the relative adsorption energies were 46.4, 37.9 and 38.6 kcal mol^{-1} based on MP2 calculations. The calculated adsorption energy is small and is insufficient to support the dissociation of H_2 on Cu(100), which does not agree with the experimental results. This may be due to the insufficiency of the neutral cluster model and failure to account

Table 3
Calculated properties of hydrogen adsorbed at the bridge, on-top and four-fold hollow sites on a Cu(100) surface

Adsorbed site	Bridge	Top	Hollow
$R_{H-surface}$ (Å)[a]	1.32	1.64	1.10
R_{H-Cu} (Å)[b]	1.83	1.64	2.12
E_{ads} (kcal mol^{-1})[c]	46.1	37.9	38.6

[a] $R_{H-surface}$ is the perpendicular distance from hydrogen to the copper surface.
[b] R_{H-Cu} is the distance from a hydrogen atom to the nearest copper atom.
[c] Adsorption energies are relative to hydrogen at infinite separation.

for surface relaxation or reorganization, the latter may play an important role in hydrogen adsorption. Note that the dissociation of H_2 on a noble metal surface is still a theoretically challenging subject, and further study is needed to understand the dissociation mechanism in more detail. Experimentally, atomic hydrogen may not be very sensitive to the adsorption site in methanol synthesis since it may occur at higher coverage or under perturbation by other coadsorbed species, and hydrogen can exhibit spillover among adsorption sites [14]. The spillover of hydrogen on a catalytic surface has been reported in practical catalytic processes [54].

Copper formate is the pivotal intermediate in methanol synthesis [5,14]. However, the structure of formate on a Cu(100) surface is controversial. Both the short-bridge site with the oxygen lying over the on-top site of the first-layer copper atoms [26] and the cross-bridge site with the oxygen lying in adjacent hollow sites [58] have been reported from extended X-ray absorption fine structure (EXAFS) studies. We compared the adsorption of formate species at different sites on the Cu(100) surface. Four adsorption sites, i.e., the short-bridge site (Fig. 9a), the on-top site (Fig. 9b), the hollow site (Fig. 9c) and the cross-bridge site (Fig. 9d), were investigated, and the results are summarized in Table 4.

For formate adsorption on the Cu(100) surface, the most stable adsorption occurs at the short-bridge site, which is consistent with previous theoretical [27–29] and experimental [26] results. The optimized C—O distance is 1.27 Å and $\angle$OCO is 125.3°, which agree well with the experimental values of 1.25 Å [26] and $129 \pm 5°$ [59] and the linear combination of atomic orbital-local density functional (LCAO-LDF) calculated values of 1.29 Å and 126° [29], respectively. The calculated Cu—O distance is 2.12 Å, which is slightly larger than the value obtained from photoelectron diffraction experiments (1.98 ± 0.04 Å) [26]. Adsorption energies are calculated to be 71.0, 63.5, 62.8 and 55.2 kcal mol^{-1} for formate adsorbed at the short-bridge, on-top, hollow and cross-bridge sites, respectively. Formate adsorbed at the short-bridge site is calculated to be 15.8 kcal mol^{-1} more stable than that adsorbed at the cross-bridge site, which is comparable to the theoretical relative energies of 9.9 kcal mol^{-1} [27], 8.8 kcal mol^{-1} [28] and 20.3 kcal mol^{-1} [29], respectively. Note that the adsorption energy was reported to be much different by different calculations [27–29], and no experimental data are available, although Taylor et al. [24] reported an estimated value of around 25 kcal mol^{-1}. Since all of the computational models that are used today in theoretical studies of chemisorptions and reactions on solid surfaces have some weaknesses, to assess the applicability of the different models it is important to make comparative studies [60]. Taking this in mind, our conclusions in this paper for the adsorptions and reaction mechanisms are mainly based on comparative results for the calculations on the same model cluster.

The geometries of the formate species adsorbed at different adsorption sites are very similar; the C—O distance is 1.27 Å and $\angle$OCO ranges from 123.3° to 125.3°. However, the Cu—O distance varies greatly. The formate at the short-bridge site has the shortest Cu—O distance and the largest adsorption energy, while that at the cross-bridge site has the longest Cu—O distance and the least stability. This means that adsorbate–surface interaction may be directly reflected by the adsorbate–surface distance for formate adsorption on a Cu(100) surface. Mulliken populations of the formate species at different adsorption sites are all about -0.53, which indicates a charge-transfer chemisorption mechanism and an anionic formate adsorption species. A similar charge-transfer chemisorption mechanism was reported for formate on Cu(100) by Mehandru and Anderson [27], and for formate on Ni(100) by Upton [61].

Table 4 also shows the calculated vibrational frequencies (VF) and the IR intensities of formate at the most stable short-bridge site, in comparison with the experimental data [24,62]. The calculation is carried out analytically by determining the second derivatives of the energy with respect to the mass-weighted coordinates at the resulting optimized geometries; i.e., the normal methods used in GAUSSIAN 94 [41]. Since HF calculations usually give overestimations, the results shown in Table 4 were obtained by multiplying the calculated values by 0.9, the average of the errors in

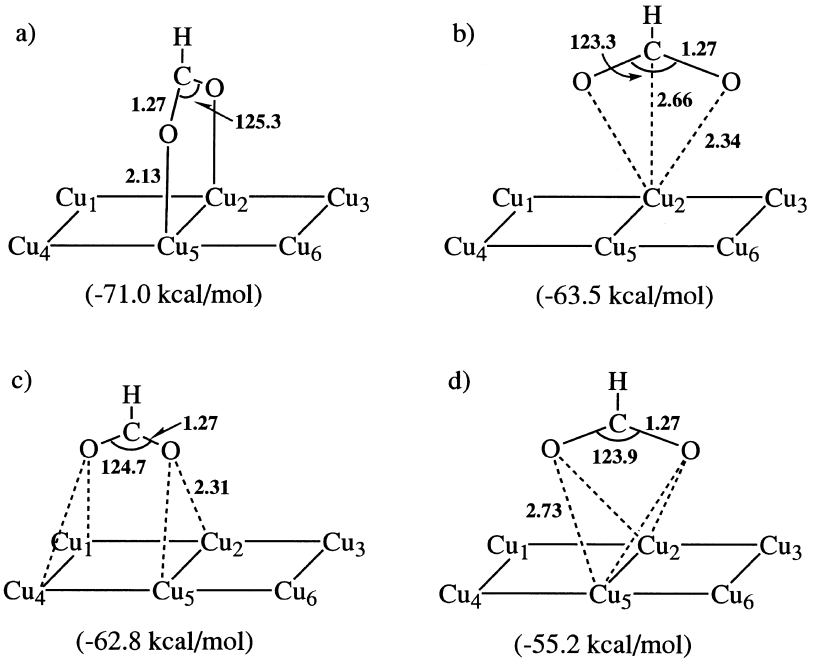

Fig. 9. Optimized geometries and adsorbed energies of formate on a Cu(100) surface. (a) Short-bridge site, (b) on-top site, (c) four-fold hollow site and (d) cross-bridge site.

Table 4
Calculated properties of formate species at different sites on a Cu(100) surface

	Short-bridge	On-top	Hollow	Cross-bridge	Experimental[a]
C—H (Å)	1.09	1.09	1.09	1.09	–
C—O (Å)	1.27	1.25	1.27	1.27	1.25
R_{O-Cu} (Å)[b]	2.13	2.34	2.40	2.73	1.98 ± 0.04
∠OCO (°)	125.3	123.3	124.8	123.9	129 ± 5
E_{ads} (kcal mol^{-1})[c]	−71.0	−63.5	−62.8	−55.2	–
Net charge	−0.526	−0.539	−0.527	−0.537	–
ν(CH)[d]	2935 (205.1)				2910
ν_s(COO)	1290 (188.6)				1330
δ(OCO)	722 (65.6)				760
ν_a(COO)	1545 (27.5)				1640
δ(CH)	1333 (0.5)				1377
π(CH)	1062 (12.9)				1073
ν_s(O—Cu)	253 (36.2)				340
ν_a(O—Cu)	225 (0.7)				

[a] From Refs. [24,26,59,62].
[b] R_{O-Cu} is the distance from the oxygen atom to the nearest copper atom.
[c] Adsorption energies are relative to HCOO at infinite separation and are calculated by MP2 method.
[d] Vibrational frequencies are in cm^{-1}: ν — stretching mode (s, symmetric; a, asymmetric); δ — in-plane deformation; π — out-of-plane deformation. IR intensities are in parentheses (km mol^{-1}). Experimental results are taken from Refs. [24,62].

VF values by HF calculations. The calculated vibrational frequencies and IR intensities, which compare well with the experimental data, indicate another important feature of formate on Cu(100). All of the asymmetric modes have smaller intensities as a result of the symmetric adsorption geometry, and the vibrational frequencies and the IR intensities are a little different than those for formate adsorbed on a Zn/Cu(100) alloy surface [63].

5.2. Coadsorption of hydrogen and CO_2: comparison of the DAM and neutral cluster model

Although CO_2 is relatively unreactive on a clean Cu(100) surface, it shows high reactivity towards coadsorbates [50]. It is generally accepted that electron donation into the antibonding orbital of CO_2 is the origin of its reactivity, and bent anionic chemisorbed CO_2^- is the precursor for formate formation [24,64]. We examined the coadsorption of hydrogen and CO_2 on a Cu(100) surface using the DAM and the neutral cluster model (CM). Fig. 10 shows the optimized coadsorption geometries and Table 5 shows the coadsorption energy and Mulliken populations.

The DAM describes chemisorbed CO_2^- on a copper surface. In the chemisorption state, about one (0.76) electron is transferred from the bulk metal into the π^* orbital of CO_2, giving a bent anionic CO_2^- species on the surface. The C—O and O—Cu bond distances are calculated to be 1.25 and 2.15 Å, respectively. Note that the gas-phase CO_2 has a C—O distance of 1.17 Å. The coadsorption energy is calculated to be 17.4 kcal mol^{-1}. Experimentally, the adsorption energy was reported to be 4.3 kcal mol^{-1} [65] for physisorbed CO_2 on a polycrystalline copper surface, 6.7 kcal mol^{-1} [24] for physisorbed CO_2 on a clean Cu(100) surface, and 14.3 kcal mol^{-1} [64] for chemisorbed CO_2 on a polycrystalline copper surface. No experimental data are available for coadsorption species. Mulliken populations show that the net charge on the adsorbed species is −0.76. This value is less than unity because of covalent interactions between the CO_2 molecular orbitals and the copper 4s-3d orbitals. The charge distribution of the metals is almost unchanged compared with that of the free cluster. In the CO_2^- adsorbate, electron transfer causes a large frontier density (spin population) on carbon, while the frontier densities on other atoms are almost zero. This large frontier density on carbon means that the carbon becomes very reactive in the adsorption state and should be the active site towards the reaction with other coadsorbates.

On the other hand, the Cu_8 cluster model does not describe the coadsorption of hydrogen and CO_2 on a Cu(100) surface naturally. It is 10.2 kcal mol^{-1} more unstable, and the geometry of the CO_2 is almost the same as that in the gas phase. If we suppose the transfer of one electron from the cluster metals to CO_2, the chemisorbed CO_2^- structure is obtained, as shown in Fig. 10c, which is similar to that in Fig. 10a calculated by the DAM. However, this structure is calculated to

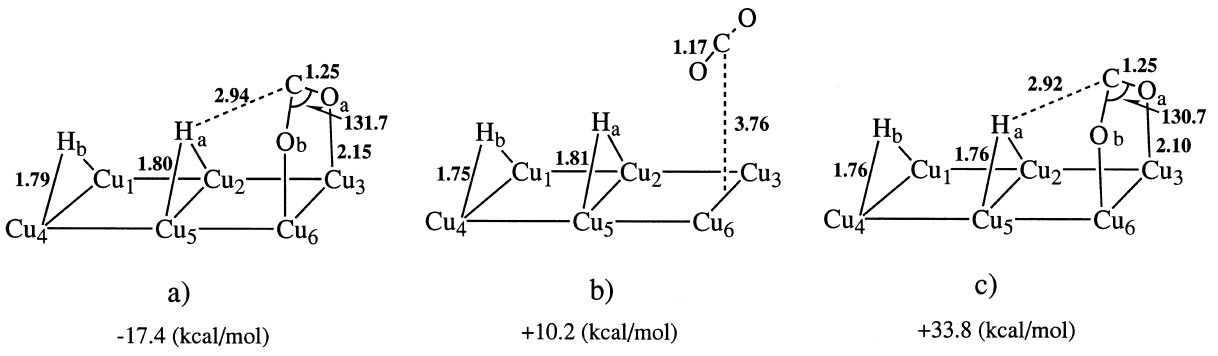

Fig. 10. Optimized geometries and coadsorbed energies of hydrogen and CO_2 on a Cu(100) surface. (a) Is calculated by the dipped adcluster model ($n=1$); (b) and (c) are calculated by the neutral cluster model ($n=0$). Detailed explanations are given in the text.

Table 5
Coadsorbed energies, Mulliken populations and frontier densities (spin populations) of coadsorbed CO_2 and hydrogen on a Cu(100) surface. The geometries are shown in Fig. 10

	Free phase	DAM	CM	
E_{ads} (kcal mol^{-1})[a]	0.0	−17.4	+10.2	+33.8
Mulliken population				
Cu_1	0.045	−0.006	0.128	0.334
Cu_2	0.016	−0.077	0.095	0.008
Cu_3	0.045	0.180	−0.043	0.266
Cu_4	0.045	−0.006	0.128	0.334
Cu_5	0.016	−0.077	0.095	0.008
Cu_6	0.045	0.180	−0.043	0.266
Cu_7	−0.105	−0.271	−0.151	−0.356
Cu_8	−0.105	−0.204	0.061	−0.078
C	0.313	0.114	0.318	0.164
O_a	−0.157	−0.344	−0.147	−0.354
O_b	−0.157	−0.344	−0.147	−0.354
H_a	0.0	−0.067	−0.069	−0.087
H_b	0.0	−0.119	−0.106	−0.152
Adsorbate[b]	0.0	−0.76	−0.199	−0.783
Frontier density				
Cu_1		−0.052		+0.095
Cu_2		+0.030		−0.444
Cu_3		+0.096		−0.238
Cu_4		−0.052		+0.095
Cu_5		+0.030		−0.444
Cu_6		+0.096		−0.238
Cu_7		+0.079		−0.098
Cu_8		−0.031		+0.164
C		+0.697		+0.725
O_a		+0.091		+0.071
O_b		+0.091		+0.071
H_a		+0.006		+0.010
H_b		−0.080		+0.229

[a] $E_{ads} = E(Cu_8 \text{ cluster–adsorbate}) - E(Cu_8 \text{ cluster}) - E(H_{2(g)}) - E(CO_{2(g)})$.
[b] Adsorbate: total net charge of the adsorbates.

be 33.8 kcal mol^{-1} more unstable, and the net charge and the frontier density of the cluster metals are quite large. The cluster is then quite unstable due to the large polarization, which explains the large negative adsorption energy for the chemisorbed CO_2^- on the neutral cluster.

The above comparative calculations show that the cluster model is insufficient for describing the coadsorption and reaction of H_2 and CO_2 on metal surfaces, since the effect of electron transfer from the bulk metal to the adsorbates cannot be adequately described and a positive adsorption energy can not be obtained. A similar situation was also observed in the adsorption of oxygen on a silver surface: a negative adsorption energy was reported even with an Ag_{24} cluster [66], while the DAM gave a reasonable adsorption energy [33–35]. Thus, the DAM is essential for theoretical studies of surface reactions in which electron transfer from the bulk metal to adsorbates is important.

6. Conclusion

In this study, we examined the mechanism of the hydrogenation of CO_2 to methanol on a

Cu(100) surface. We performed both ab initio HF and MP2 calculations using the dipped adcluster model (DAM), which takes into account the interaction between the bulk metal and admolecules by considering the electron transfer and image force between them.

The most important results are shown in Section 3, in which the reaction route and energetics of the hydrogenation of CO_2 to methanol on a Cu(100) are presented and discussed. The process involves five successive hydrogenation steps, as shown in Figs. 2 and 3. The coadsorption of hydrogen and chemisorbed CO_2^- was successfully described by the DAM, but not by the neutral cluster model. In the chemisorption state, the transfer of one electron from the bulk metal into the π^* orbital of CO_2 leads to a bent anionic CO_2^- species at the surface whose carbon atom is highly activated, and the reaction of adsorbed atomic hydrogen with coadsorbed CO_2^- readily leads to surface formate.

Formate is adsorbed at the short-bridge site with its molecular plane perpendicular to the metal surface. The calculated Cu—O distance is 2.12 Å, the C—O distance is 1.27 Å and $\angle$OCO is 125.3°. This is a stable intermediate in this reaction process. The adsorbed formate reacts with a coadsorbed atomic hydrogen to form surface dioxomethylene, which is the key intermediate in this series of surface reactions. The reaction of adsorbed dioxomethylene with adsorbed atomic hydrogen leads to surface formaldehyde. The activation energy is 17.0 kcal mol^{-1}, and the reaction is exothermic by 35.7 kcal mol^{-1}. These two steps, i.e., from formate to formaldehyde, constitute the rate-limiting step of this reaction.

Dioxomethylene is an unstable intermediate on the Cu(100) surface, but formaldehyde and methoxy intermediates are quite stable. The adsorbed formaldehyde intermediate is highly reactive towards coadsorbed atomic hydrogen, and its hydrogenation into adsorbed methoxy occurs readily. The resulting adsorbed methoxy undergoes further hydrogenation into methanol.

Our results indicate that chemisorbed CO_2^-, formate, dioxomethylene, formaldehyde and methoxy are the main intermediates in methanol synthesis. The hydrogenation of adsorbed formate to adsorbed dioxomethylene has the highest energy barrier of 23.0 kcal mol^{-1}, and is endothermic by 17.1 kcal mol^{-1}. The DAM is essential for the theoretical study of the chemisorption and reaction mechanism of this surface process.

Acknowledgements

We are grateful to Dr J. Nakamura at the University of Tsukuba. Some calculations were performed using the computers at the Institute for Molecular Science. Part of this study was supported by a Grant-in-Aid for Scientific Research from the Japanese Ministry of Education, Science, and Culture, and by a grant from the Kyoto University VBL project.

References

[1] M. Saito, Shokubai 35 (1993) 485 in Japanese.
[2] C.G. Chinchen, P.J. Denny, J.R. Jennings, M.S. Spencer, K.C. Waugh, Appl. Catal. 36 (1988) 1.
[3] M. Bowker, H. Houghton, K.C. Waugh, J. Chem. Soc., Faraday Trans. 77 (1981) 3023.
[4] G.C. Chinchen, P.J. Denny, D.G. Parker, M.S. Spencer, K.C. Waugh, D.A. Whan, Appl. Catal. 30 (1987) 333.
[5] G.J. Millar, C.H. Rochester, K.C. Waugh, Catal. Lett. 14 (1992) 289.
[6] K. Klier, Adv. Catal. 31 (1982) 243.
[7] Y. Okamoto, K. Fukino, T. Imanaka, S. Teranishi, J. Phys. Chem. 87 (1983) 3747.
[8] T. Fujitani, I. Nakamura, T. Uchijima, J. Nakamura, Surf. Sci. 285 (1994) 285.
[9] Y. Kanai, T. Watanabe, T. Fujitani, T. Uchijima, J. Nakamura, Catal. Lett. 38 (1996) 157.
[10] J. Nakamura, I. Nakamura, T. Uchijima, Y. Kanai, T. Watanabe, M. Saito, T. Fujitani, J. Catal. 160 (1996) 65.
[11] T. Kakumoto, Energy Convers. Mgmt. 36 (1995) 661.
[12] R. Burch, R.J. Chappell, S.E. Golunski, J. Chem. Soc., Faraday Trans. 85 (1989) 3569.
[13] R. Burch, S.E. Golunski, M.S. Spencer, J. Chem. Soc., Faraday Trans. 86 (1990) 2683.
[14] R. Burch, S.E. Golunski, M.S. Spencer, Catal. Lett. 5 (1990) 55.
[15] S.G. Neophytides, A.M. Marchi, G.F. Froment, Appl. Catal. A 86 (1992) 45.
[16] J.B. Friedrich, D.J. Young, M.S. Wainwright, J. Catal. 80 (1983) 14.
[17] J.S. Szanyi, W. Goodman, Catal. Lett. 10 (1991) 383.
[18] P.B. Rasmussen, M. Kazuta, I. Chorkendorff, Surf. Sci. 318 (1994) 267.

[19] P.B. Rasmussen, P.M. Holmblad, T. Askgaard, C.V. Ovesen, P. Stoltze, J.K. Nørskov, I. Chorkendorff, Catal. Lett. 26 (1994) 373.
[20] J. Yoshihara, S.C. Parker, A. Schafer, C.T. Campbell, Catal. Lett. 31 (1995) 313.
[21] J. Yoshihara, C.T. Campbell, J. Catal. 161 (1996) 776.
[22] A. Kiennemann, J. Idriss, J.P. Hindermann, J.C. Lavalley, A. Vallet, P. Chaumette, P.H. Courty, Appl. Catal. 59 (1990) 165.
[23] M. Bowker, R.A. Hadden, H. Houghton, J.N. Hyland, K.C. Waugh, J. Catal. 109 (1988) 263.
[24] P.A. Taylor, P.B. Rasmussen, C.V. Ovesen, P. Stoltze, I. Chorkendorff, Surf. Sci. 261 (1992) 191.
[25] J. Onsgaard, S.V. Christensen, P.J. Godowski, J. Nerlov, S. Quist, Surf. Sci. 370 (1997) L137.
[26] D.P. Woodruff, C.F. McConville, A.L.D. Kilcoyne, Th. Linder, J. Somers, M. Surman, G. Paolucci, A.M. Bradshaw, Surf. Sci. 201 (1988) 228.
[27] S.P. Mehandru, A.B. Anderson, Surf. Sci. 219 (1989) 68.
[28] A. Wander, B.W. Holland, Surf. Sci. 199 (1988) L403.
[29] M. Casarin, G. Granozzi, M. Sambi, E. Tondello, A. Vittadini, Surf. Sci. 307 (1994) 95.
[30] H. Nakatsuji, J. Chem. Phys 87 (1987) 4995.
[31] H. Nakatsuji, H. Nakai, Y. Fukunishi, J. Chem. Phys. 95 (1991) 640.
[32] H. Nakatsuji, Prog. Surf. Sci. 54 (1997) 1.
[33] H. Nakatsuji, H. Nakai, Chem. Phys. Lett. 174 (1990) 283.
[34] H. Nakatsuji, H. Nakai, Can. J. Chem. 70 (1992) 404.
[35] H. Nakatsuji, H. Nakai, J. Chem. Phys. 98 (1993) 2423.
[36] H. Nakatsuji, H. Nakai, K. Ikeda, Y. Yamamoto, Surf. Sci. 384 (1997) 315.
[37] H. Nakatsuji, K. Takahashi, Z-.M. Hu, Chem. Phys. Lett. 277 (1997) 551.
[38] H. Nakatsuji, Z-.M. Hu, H. Nakai, Int. J. Quantum Chem. 65 (1997) 839.
[39] Z-.M. Hu, H. Nakai, H. Nakatsuji, Surf. Sci. 401 (1998) 371.
[40] H. Nakatsuji, Z-.M. Hu, H. Nakai, K. Ikeda, Surf. Sci. 387 (1997) 328.
[41] M.J. Frish, G.W. Trucks, H.B. Schlegel, P.M.W. Gill, B.G. Johnson, M.A. Robb, J.R. Cheeseman, T.A. Keith, G.A. Petersson, J.A. Montgomery, K. Raghavachari, M.A. Al-Laham, V.G. Zakrzewski, J.V. Ortiz, J.B. Foresman, J. Cioslowski, B.B. Stefanov, A. Nanayakkara, M. Challacombe, C.Y. Peng, P.Y. Ayara, W. Chen, M.W. Wong, J.L. Andres, E.S. Replogle, R. Gomperts, R.L. Martin, D.J. Fox, J.S. Binkley, D.J. Defrees, J. Baker, J.P. Stewart, M.. Head-Gordon, C. Gonzalez, J.A. Pople, Gaussian 94 (Revision E.2), Gaussian Inc, Pittsburgh, PA, 1995.
[42] P.J. Hay, W.R. Wadt, J. Chem. Phys. 82 (1985) 270.
[43] S. Huzinaga, J. Chem. Phys. 42 (1965) 1293.
[44] T.H. Dunning Jr., J. Chem. Phys. 53 (1970) 2823.
[45] S. Huzinaga, J. Andzelm, M. Kiobukowski, E.. Radzio-Andzelm, Y. Sakai, H. Tatewaki, Gaussian basis sets for molecular calculations, in: Physical Science Data vol. 16, Elsevier, Amsterdam, 1984, p. 23.
[46] G. Wiesenekker, G.J. Kroes, E.J. Baerends, J. Chem. Phys. 104 (1996) 7344.
[47] M. Bowker, R.J. Madix, Surf. Sci. 102 (1981) 542.
[48] M. Bowker, R.J. Madix, Surf. Sci. 95 (1980) 190.
[49] B.A. Sexton, Surf. Sci. 88 (1979) 299, 319.
[50] H.J. Freund, M.W. Roberts, Surf. Sci. Rep. 25 (1996) 225.
[51] T. Tagawa, N. Nomura, M. Shimakage, S. Goto, Res. Chem. Intermed. 21 (1995) 193.
[52] D.K. Lee, D.S. Kim, C.M. Yoo, C.S. Lee, I.C. Cho, in: T. Inui, M. Anpo, K. Izui, S. Yanagida, T. Yamaguchi (Eds.), Advances in Chemical Conversions for Mitigating Carbon Dioxide, Elsevier Science BV, New York, 1998, p. 509.
[53] I. Chorkendorff, P.A. Taylor, P.B. Rasmussen, J. Vac. Sci. Technol. A 10 (1992) 2277.
[54] W.C. Conner Jr., J.L. Falconer, Chem. Rev. 95 (1995) 759.
[55] Z.-M. Hu, H. Nakatsuji, Surf. Sci. 425 (1999) 296.
[56] P.B. Rasmussen, P.M. Holmblad, H. Christofferesen, P.A. Taylor, I. Chorkendorff, Surf. Sci. 287/288 (1993) 79.
[57] J.A. White, D.M. Bird, M.C. Payne, I. Stich, Phys. Rev. Lett. 73 (1994) 1404.
[58] D.A. Outka, R.J. Madix, J. Stöhr, Surf. Sci. 164 (1985) 235.
[59] M. Sambi, G. Granozzi, M. Casarin, G.A. Rizzi, A. Vittadini, L.S. Caputi, G. Chiarello, Surf. Sci. 315 (1994) 309.
[60] L. Triguero, U. Wahlgren, L.G.M. Pettersson, P. Siegbahn, Theor. Chim. Acta 94 (1996) 297.
[61] T.H. Upton, J. Chem. Phys. 83 (1985) 5084.
[62] B.A. Sexton, Surf. Sci. 88 (1979) 319.
[63] Z.-M. Hu, H. Nakatsuji, Chem. Phys. Lett., in press.
[64] R.G. Copperthwaite, P.R. Davies, M.A. Morris, M.W. Roberts, R.A. Ryder, Catal. Lett. 1 (1988) 11.
[65] R.A. Hadden, H.D. Vandervell, K.C. Waugh, G. Webb, Catal. Lett. 1 (1988) 27.
[66] T.H. Upton, P. Stevens, R.J. Madix, J. Chem. Phys. 88 (1988) 3988.
[67] K.P Huber, G. Herzberg, Molecular Spectra and Molecular Structure IV. Constants of Diatomic Molecules, Van Nostrand Reinhold, New York, 1979.
[68] C.E. Moore, in: NSRDS-NBS 35, Atomic Energy Levels vol. II, National Bureau of Standards, Washington, DC, 1971, p. 112.
[69] T. Inui, in: S. Inoue, K. Izui, K. Tanaka (Eds.), Carbon Dioxide Chemistry Biochemistry and Environment, Tokyo Kagaku Doujin Press, Tokyo, 1994, p. 79. in Japanese.